Article

Co-Optimization of Communication and Sensing for Multiple Unmanned Aerial Vehicles in Cooperative Target Tracking

Zhong Liu [ID] **, Xiaowei Fu * ** [ID] **and Xiaoguang Gao**

School of Electronics and Information, Northwestern Polytechnical University, Xi'an 710072, China;
15829732829@163.com (Z.L.); cxg2012@nwpu.edu.cn (X.G.)

* Correspondence: fxw@nwpu.edu.cn; Tel.: +86-029-8843-1260

check for updates

Abstract: In this paper, we consider motion-planning for multiple unmanned aerial vehicles (UAVs) that oversee cooperative target tracking in realistic communication environments. We present a novel multi-UAVs cooperative target tracking algorithm based on co-optimization of communication and sensing strategy, which can generate information-gathering trajectories considering the multi-hops communication reliability. Firstly, a packet-erasure channel model is used to describe the realistic wireless communication links, in which the probability of a successful information transmission is modeled as a function of the signal-to-noise ratio (SNR). Secondly, the Fisher information matrix (FIM) is used to quantify the information gained in target tracking. Thirdly, a scalar metric is used for trajectories panning over a finite time horizon. This scalar metric is a utility function of the expected information gain and the probability of a successful information transmission. With the combining of the sensing and communication into a utility function, the co-optimization of communication and sensing is reflected in the tradeoffs between maximizing information gained and improving communication reliability. The results of comparison simulations show that the proposed algorithm effectively improved estimation performance compared to the method that does not consider communication reliability.

Keywords: multi-UAVs; cooperative target tracking; information filter; radio frequency communication; Fisher information matrix; receding horizon optimizing

1. Introduction

Recently, multiple unmanned aerial vehicles (UAVs) have received increasing attention for their accomplishments in both military and civil applications. Tracking of a moving ground target is one of the important applications of UAVs, with the aim of increasing the overall knowledge of the target's state (position, velocity, etc.) and taking proactive measures. The goal of cooperative target tracking is to control multiple UAVs to keep tracking a moving target and obtain more accurate target state estimates.

In cooperative target tracking missions two or more UAVs track the same target. Under such a mission two main technical issues arise [1]: (1) Target motion estimation; each UAV has a local estimation of the target state (position and velocity). To obtain a more accurate target state estimate, it is necessary to develop global estimation strategies by fusing the local estimates from UAVs in an efficient manner; (2) Observer trajectory optimization; by developing cooperative control methods, UAVs can move in such a way as to minimize the error and uncertainty of the target state estimation. Extensive studies have been carried out on these two key issues.

Target-motion estimation has been a major problem in the field of target tracking and has received great attention. In target tracking applications, sensors (such as camera, radar, and sonar, etc.) installed on the UAVs can obtain measurements, such as the relative range and azimuth of the target with respect to the position of the airborne UAV. According to the measurement data, the UAV can obtain a target state estimate which generally is suboptimal given the local information. Fortunately, the communication capabilities of the UAVs enable sending their measurement data to a fusion center (e.g., base station), which leads to a global optimal estimate. Most of existing estimation and fusion methods are based on the information filter (IF), which is the information form of the Kalman filter (KF). For the IF, the information vector and matrix are employed instead of the mean and covariance used in the standard KF to represent the Gaussian distribution [2–4]. In this way, the IF has advantages to handle sensor fusion tasks and unknown prior covariance conditions. Thus, IF is more widely used than KF in the estimation and fusion problems for multiple sensors [5,6]. Ridley [7] provides a decentralized airborne data fusion method based on the IF for ground targets tracking. Casbeer [8] presented a new information consensus filter (ICF) for distributed dynamic-state estimation, in which estimation is handled by the traditional information filter, while the communication of measurements is handled by a consensus filter. Additionally, the unscented information filter (UIF) has been proposed for distributed estimation with nonlinear dynamics. Lin [9] presented an adaptive consensus-based distributed UIF for mobile sensor networks with communication delays. These studies show that the IF and its extensions can effectively solve the problem of data fusion from different sensor platforms.

The observer trajectory optimization problem focuses on determining the trajectories of multiple UAVs (note, the UAVs are the observers) such that the target state estimation error is minimized. This issue is concerned with the cooperative control of the movements of multiple UAVs to guarantee the optimal observer trajectory for target motion estimation. Different earlier studies have developed observer trajectory planning approaches, including the gradient-based control law [10,11], Lyapunov vector fields (LVF) [12,13], and receding horizon optimization (RHO) [14,15], among others. In References [10,11], an optimal sensing strategy was given by minimizing the determinant of the estimation error covariance matrix, and a gradient-based control law was derived for each sensor platform to reach a local optimum. However, kinematic constraints of the platform were not considered, and this gradient-based control strategy was easily trapped in local optimal solutions. Frew [12] introduced Lyapunov guidance vector fields in an approach that maintains a prescribed standoff radius. Additionally, Oh [13] proposed a coordinated standoff tracking method for groups of moving targets using multiple UAVs. The vector field guidance approach was applied to track a group of targets for a single UAV by defining a variable standoff orbit, to be followed, which keeps all targets within the field-of-view of the UAV. However, their study neglected the accuracy of target motion estimation in the tracking process.

Target motion estimation is a dynamic process and as a result, the performance of the estimation depends on the trajectory of the sensor platform. To generate observer trajectories that improve the performance of the target-motion estimation, several observer trajectory planning methods that are based on receding horizon optimizing have been proposed. For example, Ponda [14] presented an information theoretic approach for vehicle trajectory optimization in the 3D bearings-only target localization problem. The trace of the Fisher information matrix (FIM) was used as the quality metric for assessing the estimation performance and gave a framework for the choice of vehicle trajectories that increased the information provided by the measurements to improve the accuracy of the estimation. In Reference [15], a receding horizon control scheme for trajectory planning in target tracking was presented for the problem of cooperative persistent target tracking in an urban environment. In that study, the tracking objective was to maximize the information contribution from each UAV.

In cooperative target tracking missions, each UAV must process the measurement results received from others to improve its estimate, and thus communication plays a key role in target tracking. However, most of current researches assume ideal or non-realistic communication and

consider only sensing objectives. For instance, it is common to assume either perfect links or links that are perfect within a certain radius, a significant over-simplification of communication links. Wireless transmission is degraded by several factors such as path loss, shadowing, fading, and noise. Therefore, considering the impact of communication on estimation and control is an emerging area of research [16]. Reference [17] investigated how to use the UAVs to build up a communication network rapidly in a disaster environment. The deployment of the UAVs is optimized such that a line-of-sight situation is achieved as well as a minimum required signal-to-noise ratio being ensured at the receivers. However, the scenario in this literature is static, and the method is cannot be directly applied to the moving target tracking scenario that is considered in this paper. The problem of integrating communication and sensing together for information gathering tasks is treated in Reference [18]. The approach of [18] optimizes information metric over a finite horizon which accounts for the qualities of communication links between the UAVs. In the scenario, once the range is too large for direct communication to the base station, some UAVs act as communication relays to maintain connectivity and further improve performance. Therefore, the UAVs automatically establish fixed multi-hop chains to get the measurements back to the base station. In this the fixed communication topology, the formation of the UAVs is rigid [19]. The rigid formation has higher stability, because the only permissible smooth motions are translations or rotations of the entire formation. However, due to the fixed communication topology, the algorithms do not produce efficient results in the dynamic scenario of moving target tracking.

From these earlier studies it is clear that the motion decisions of each UAV should consider both the information gained through its sensor as well as communication with fusion center. This creates a multi-objective optimization problem where communication and sensing are both optimized such that each UAV chooses a trajectory that gives the best balance between its communication and sensing. A trajectory only maximizing sensing capabilities may not guarantee effective communication performance, while a trajectory that optimizes communication may result in poor sensing. Thus, the co-optimization of communication and sensing is reflected in the tradeoffs between maximizing information gained and improving communication reliability.

In this paper, we study the problem of multiple UAVs cooperative tracking a moving target. The main contribution of this paper is to develop a motion planning algorithm in which communication and sensing are both optimized. Our novel motion planning approach properly integrates the communication and sensing objectives to accomplish the target tracking mission of multiple UAVs, while maintaining proper connectivity to the remote base station.

The structure of this paper is organized as follows. In Section 2, the mission scenario and the problem formulation is provided. Section 3 discusses the extended information filter (EIF) and the sensor fusion algorithms for moving target tracking in realistic communication environment. This section also introduces the Fisher Information Matrix (FIM), which is the inverse of Cramer-Rao Lower Bound (CRLB), as a tool to measure estimation performance. By identifying the measure of estimation performance, an observer trajectory quality metric is developed which can be used to determine the optimal trajectories of the UAVs for tracking a moving target. This trajectory quality metric combines the communication and sensing into a utility function. In Section 4, we propose our motion planning algorithm based on co-optimization of communication and sensing. The motion planning is performed in a distributed fashion, i.e., each UAV solves local rolling time domain optimization problem and obtains its own trajectory. We present our simulation and experimental results in Section 5, followed by summary and conclusions in Section 6.

2. Problem Formulation and Model

Consider a fixed remote base station which uses N homogeneous UAVs for tracking a moving ground target, as shown in Figure 1. Each UAV is identified by a unique identity number A_i, $i = 1, 2, \ldots, N$, and is equipped with a moving target indicator radar (MTIR) to localize the position of the target by measuring the relative distance and azimuth with respect to the UAV's own position. With the MTIR measurement,

each UAV executes the filter algorithm and obtains its local estimation of the target state (position and velocity). However, since a single local estimate is suboptimal, each UAV sends its local estimate to the remote base station for fusion which enhances the tracking accuracy. After the base station receives all the UAVs' local estimates via the communication links, a global optimal estimate of the target state is obtained with the fusion algorithm. The overall goal is for the station to constantly have a good global estimate of the target state. However, the communication links between the UAVs and the base station are affected by path loss, shadowing, fading, and noise, which can drastically degrade the quality of the received information.

In this paper, we employ a packet-erasure channel model to describe the realistic wireless communication links. That is to say, the base station will drop all the packets with a received signal-to-noise ratio (SNR) below a predefined threshold. Please note that in practice, more distance between two communication nodes results in a lower received SNR. In this case, these two communication nodes might be regarded as disconnected. Thus, for a UAV that is far away from the base station, it fails to communicate with the base station directly. To ensure that the UAV can send its local estimation results to the remote base station, some other UAVs act as communication relays to maintain connectivity. The quality of the links should be considered in motion-planning such that the UAVs intelligently move to locations that maximize both the information gain and the successful transmission probabilities in communication links with the base station.
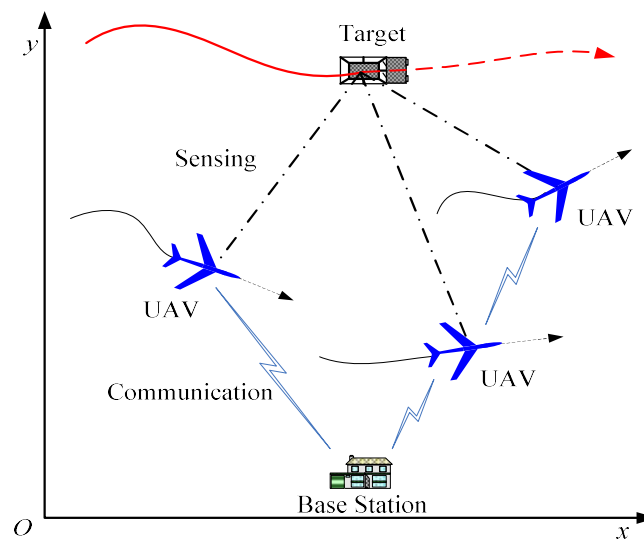

Figure 1. The scenario where a fixed base station utilizes multi-UAVs for tracking a ground moving target.

2.1. UAV Dynamical Model

For simplicity, it is assumed that each UAV is equipped with a low-level flight control system [20–23] that holds constant altitude and speed. A general flight control system—which includes the attitude angles (roll, pitch, and yaw) controller and fast loop attitude angle rates controller—can follow the guidance inputs to generate control surface deflections. In general, the guidance inputs include the speed (v), the vertical flight path angle (γ) and the horizontal flight path angle (χ). In this paper, we assume that the UAVs move on a fixed altitude with a constant cruising speed. Thus, we only need to designate the horizontal flight path angle (χ^c), which is the sole guidance input to this low-level flight control system. The two-dimension motion of a UAV in a horizontal plane is thus described by:

$$\begin{pmatrix} \dot{x}_i \\ \dot{y}_i \\ \dot{\chi}_i \end{pmatrix} = f(x_i, u_i) = \begin{pmatrix} v_i \cos \chi_i \\ v_i \sin \chi_i \\ \alpha_\chi (\chi_i^c - \chi_i) \end{pmatrix} \tag{1}$$

where $x_i = [x_i, y_i, v_i, \chi_i]^T$ denotes the x and y components of the planar position, the speed, and the horizontal flight path angle of UAV A_i, respectively. Additionally, α_χ is the control gain, and $u_i = \chi_i^c$ is the desired horizontal flight path angle of A_i, which is the guidance input for the low-level flight control system of the UAV. $\dot{\chi}_i$ is the turning rate, which is constrained by the following dynamic limits:

$$-\omega_{max} \le \dot{\chi}_i \le \omega_{max} \tag{2}$$

The continuous UAV model in Equation (1) can be discretized by Euler integration method:

$$x_i(k+1) = f_u(x_i(k), u_i(k)) = x_i(k) + T_s f(x_i(k), u_i(k)) \tag{3}$$

where T_s is the discrete sampling time.

2.2. Target Dynamical Model

Due to the ground target move with much lower speeds than UAVs, we use a constant-velocity target model in this paper. This constant-velocity target model regards the target acceleration as a zero-mean Gaussian acceleration noise. Therefore, we define $x_t(k) = [x_t(k), v_t^x(k), y_t(k), v_t^y(k)]^T$, with $p_t(k) = [x_t(k), y_t(k)]^T$ and $v_t(k) = [v_t^x(k), v_t^y(k)]^T$ to denote the target position and velocity at time k, respectively. The discrete model of the moving target is thus expressed by:

$$x_t(k+1) = f_t(x_t(k), w(k)) = F(k)x_t(k) + G(k)w(k) \tag{4}$$

where $w(k) \sim N(0, Q(k))$ represents the dynamic acceleration noise. The covariance matrix of the process noise $w(k)$ is $Q(k) = \text{diag}(\delta_x^2(k), \delta_y^2(k))$. $\delta_x(k)$ and $\delta_y(k)$ are the standard deviations related to target acceleration toward x and y axes. The state transition matrix $F(k)$ and the process noise input matrix $G(k)$ are expressed as:

$$F(k) = \begin{bmatrix} 1 & T_s & 0 & 0 \\ 0 & 1 & 0 & 0 \\ 0 & 0 & 1 & T_s \\ 0 & 0 & 0 & 1 \end{bmatrix} G(k) = \begin{bmatrix} \frac{T_s^2}{2} & T_s & 0 & 0 \\ 0 & 0 & \frac{T_s^2}{2} & T_s \end{bmatrix}^T \tag{5}$$

2.3. Sensor Model

In this paper, each UAV is equipped with a moving target indicator radar (MTIR) to localize the position of the target. In the MTIR, the sensor measurement $z_i(k)$ is composed of the relative range, $\tilde{r}_i(k)$, and azimuth, $\tilde{\theta}_i(k)$, of the target with respect to the position of the airborne UAV. Using the target position $x_t(k)$ and the UAV position $x_i(k)$, the sensor measurement is defined via:

$$\begin{aligned} z_i(k) &= \begin{bmatrix} \tilde{r}_i(k) \\ \tilde{\theta}_i(k) \end{bmatrix} = h_i(k, x_i(k), x_t(k)) + v_i(k) \\ &= \begin{bmatrix} \sqrt{(x_t(k) - x_i(k))^2 + (y_t(k) - y_i(k))^2} \\ \arctan\frac{y_t(k) - y_i(k)}{x_t(k) - x_i(k)} \end{bmatrix} + v_i(k) \end{aligned} \tag{6}$$

In Equation (6), $v_i(k) \sim N(0, R_i(k))$ is the measurement noise, and its covariance matrix $R_i(k) = \text{diag}(\delta_r^2(k), \delta_\theta^2(k))$; $\delta_r(k)$ and $\delta_\theta(k)$ are the standard deviations of range and azimuth, respectively. Let the matrix $H_i(k) \cdot$ be the Jacobian of the nonlinear function $h_i(k, x_i(k), x_t(k))$ with respect to the target state $x_t(k)$:

$$H_i(k) = \begin{bmatrix} \cos\theta_i(k) & 0 & \sin\theta_i(k) & 0 \\ -\frac{\sin\theta_i(k)}{r_i(k)} & 0 & \frac{\cos\theta_i(k)}{r_i(k)} & 0 \end{bmatrix} \tag{7}$$

Thus, Equation (6) can be rewritten in terms of the following linear equation:

$$z_i(k) = H_i(k) \cdot x_t(k) + v_i(k) \tag{8}$$

2.4. Communication Model

We use a packet-erasure channel model to describe the realistic wireless communication links, in which the receiver drops all the packets with a received SNR below a predefined threshold. The received signal-to-noise ratio (SNR) Γ_{ij} at node j from a transmitting node i is given by:

$$\Gamma_{ij} = \frac{P_i G_{ij}}{N_j} \tag{9}$$

where $P_i > 0$ is the power delivered to the transmitting antenna of node i; $N_j > 0$ is the average noise power when node j operating as a receiver, and G_{ij} is the channel gain. Using the Rayleigh model, G_{ij} can be expressed as:

$$G_{ij} = \frac{C_{ij}|h_{ij}|^2}{d_{ij}^\alpha} \tag{10}$$

where C_{ij} is a constant in which the antenna gains and shadowing are considered. h_{ij} represents the multi-paths fading. The distance between nodes i and j is d_{ij}. α is the propagation loss factor. Maintaining a successful transmission with an acceptably small packet loss requires a sufficiently high received SNR. In this paper, the required SNR threshold that to obtain minimal link quality is γ. Therefore, if we assume that the channel has fast Rayleigh fading [24], the probability of a successful transmission between nodes i and j is given by:

$$P_r^{ij}(\Gamma_{ij} \geq \gamma) = \exp\left(-\frac{N_j \gamma d_{ij}^\alpha}{C_{ij} P_i}\right) \tag{11}$$

Equation (11) describes a realistic wireless communication model. Please note that a larger distance between nodes i and j results in a lower received SNR. If $\Gamma_{ij} < \gamma$, the packet from node i will be dropped by node j, and thus nodes i and j are regarded as disconnected. If $\Gamma_{ij} \geq \gamma$, the packet from node i will be successfully received by node j, and thus nodes i and j are regarded as connected. The relationship between P_r^{ij} and the distance d_{ij} is shown in Figure 2; for the parameters listed in Table 1.
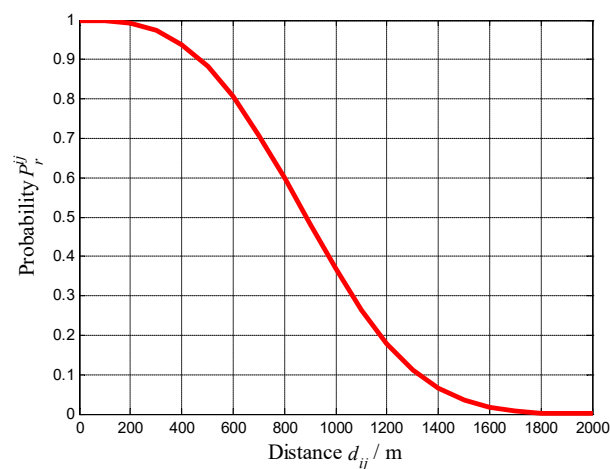

Figure 2. The probability of a successful transmission vs. distance, as determined by Equation (11) for the parameters listed in Table 1.

Table 1. The parameters of the realistic wireless communication model.

Parameter	Value	Unit
Transmission power P_i	30	dBm
Noise power N_j	−70	dBm
SNR requirement γ	10	-
Antenna gain constant C_{ij}	1	-
Propagation loss factor α	3	-

To compute the highest successful transmission probability between the source and desired destination, we should examine all possible multi-hop routes. If the successful transmission of the packet in each hop is independent, the successful transmission probability in a given multi-hop route (route$_k$) is given by:

$$P_r(\text{route}_k) = \prod_{(i,j) \in \text{route}_k} P_r^{ij} \tag{12}$$

The specific route will be chosen by the routing algorithm. In this paper, the packet routing algorithm will always choose the route with the highest successful transmission probability.

Remark 1. *In addition to the Rayleigh fading model used in our algorithm, other fading models can also be employed in a similar way. In practice, the distribution of the channels can be collected and employed within the framework of this paper in a straightforward way. In future work, we will design other communication fading models, such as Rician fading, and integrate them into the framework of co-optimization of communication and sensing.*

3. Target State Estimation and Observer Trajectory Quality Metric

3.1. Target State Estimation

Considering the advantage of using information filter in multiple sensor estimation and fusion problems, the estimation of target state is performed by using the EIF. The EIF is the information form of EKF. The EKF generates the target state estimation, $\hat{x}_t(k|k)$, at time k, together with a corresponding estimate covariance $P(k|k)$. The EIF is obtained by re-writing the target state estimate and covariance in terms of the information vector $\hat{y}$ and information matrix Y.

$$\hat{y} = P^{-1}\hat{x}_t, \ Y = (P)^{-1} \tag{13}$$

At time k, each UAV A_i runs the following EIF algorithm.

- Prediction phase

$$Y_{i,k|k-1} = (F_k Y_{i,k-1|k-1}^{-1} F_k^{\mathrm{T}} + G_k Q_k G_k^{\mathrm{T}})^{-1} \tag{14}$$

$$\hat{y}_{i,k|k-1} = Y_{i,k|k-1} F_k Y_{i,k-1|k-1}^{-1} \hat{y}_{i,k-1|k-1} \tag{15}$$

$$\hat{x}_{t,i,k|k-1} = Y_{i,k|k-1}^{-1} \hat{y}_{i,k|k-1} \tag{16}$$

- Measurement update

$$Y_{i,k|k} = Y_{i,k|k-1} + I_{i,k} \tag{17}$$

$$\hat{y}_{i,k|k} = \hat{y}_{i,k|k-1} + i_{i,k} \tag{18}$$

$$\hat{x}_{t,i,k|k} = Y_{i,k|k}^{-1} \hat{y}_{i,k|k} \tag{19}$$

where $\hat{y}_i$ and Y_i represent the information state vector and information matrix of the UAV A_i, respectively. At the time k, A_i obtains measurement $z_{i,k}$, and performs the associated information state and matrix updates

$$i_{i,k} = H_{i,k}^T R_{i,k}^{-1} \left[z_{i,k} - h_i(k, x_{i,k}, \hat{x}_{\text{t},i,k|k-1}) + H_{i,k}\hat{x}_{\text{t},i,k|k-1} \right] \tag{20}$$

$$I_{i,k} = H_{i,k}^T R_{i,k}^{-1} H_{i,k} \tag{21}$$

Since its local estimation is not perfect, each UAV must send its estimate estimation to the base station to obtain the global optimal estimate, thus enhancing the tracking accuracy of the UAVs. The base station obtains the global optimal estimate by using following fusion algorithm:

$$\hat{y}_{\text{B},k|k} = \hat{y}_{\text{B},k|k-1} + \sum_{i=1}^{N} \xi_{i,k} \cdot i_{i,k} \tag{22}$$

$$Y_{\text{B},k|k} = Y_{\text{B},k|k-1} + \sum_{i=1}^{N} \xi_{i,k} \cdot I_{i,k} \tag{23}$$

where $\hat{y}_{\text{B}}$ and Y_{B} represent the information state vector and information matrix of the base station, respectively. In Equations (22) and (23), we use $\xi_{i,k}$ to indicate whether UAV A_i has sent its own estimation to the base station successfully. $\xi_{i,k}$ is a random variable taking on either 0 or 1 from the following Bernoulli distribution

$$P(\xi_{i,k} = 1) = \beta_{i,k}; P(\xi_{i,k} = 0) = 1 - \beta_{i,k} \tag{24}$$

where $\beta_{i,k}$ indicates the probability of the packet successfully getting through from A_i to the base station. $\beta_{i,k}$ can be calculated by Equations (11) or (12).

Hence, the global optimal estimate of the target state determined by the base station is:

$$\hat{x}_{\text{t},k|k} = \left(Y_{\text{B},k|k} \right)^{-1} \cdot \hat{y}_{\text{B},k|k} \tag{25}$$

3.2. Observer Trajectory Quality Metric

A metric is defined in this section which can be used to determine the optimal trajectories of the UAVs for tracking a moving target. In practice, the performance of target-motion estimation depends on the trajectories of the UAVs. That is, the performance of target-motion estimate is a function of the specific observer trajectory, and therefore some trajectories lead to better performance (accuracy, effectiveness, etc.) than others. The goal of the cooperative target tracking mission is to enhance the global estimate performance by determining optimal or near-optimal observer trajectories. To generate good trajectories, it is necessary to define the notion of quality metric for the global estimate of target state. Therefore, the problem of identifying the best trajectory-quality metric is the problem of determining the best description of estimation performance.

According to the Cramer–Rao lower bound (CRLB) theorem, the estimation error covariance represents the uncertainty associated with the accuracy of the estimation results, which should be minimized. The CRLB provides a lower bound for the error covariance and any unbiased estimator that achieves this lower bound is considered efficient. Specifically:

$$P_k = \text{E}[(\hat{x}_{\text{t},k} - x_{\text{t},k})(\hat{x}_{\text{t},k} - x_{\text{t},k})^\text{T}] \geq C_k = Y_k^{-1} \tag{26}$$

where $x_{\text{t},k}$ is the target state to be estimated, $\hat{x}_{\text{t},k}$ is the unbiased estimate of $x_{\text{t},k}$ given the measurements z_k, and P_k represents the covariance of the estimation error. The CRLB on P_k is denoted by C_k and its inverse $Y_k = (C_k)^{-1}$ is the Fisher information matrix (FIM).

CRLB provides a lower bound on the achievable covariance of the estimator. It means minimizing the covariance of the estimation can be achieved by minimizing CRLB. Minimizing the covariance of the estimation will reduce the uncertainty of the estimation results, and then improve the estimator performance. Since the CRLB and the FIM are inversely related, maximizing the FIM will improve the estimator performance and reduce uncertainty. Thus, the optimal sensing trajectory can be generated by maximizing the FIM.

According to References [14,18], the FIM can be predicted at future time $(k + l)$, based on the current target state estimation results. Prediction of FIM, $\hat{Y}_{k+l|k}$, is computed via the following recursive form

$$\hat{Y}_{k+l|k} = \left(F_{k+l-1} \hat{Y}_{k+l-1|k}^{-1} F_{k+l-1}^{\mathrm{T}} + G_{k+l-1} Q_{k+l-1} G_{k+l-1}^{\mathrm{T}} \right)^{-1} + \hat{I}_{k+l|k} \tag{27}$$

where the recursive equation starts with $\hat{Y}_k = Y_{k|k}$. The matrix $\hat{I}_{k+l|k}$ is the prediction of the information gain matrix, which is regarded as the expected measurement contribution to the FIM from all the UAVs. On one hand, $\hat{I}_{k+l|k}$ is dependent on the planned trajectories of all the UAVs. On the other hand, $\hat{I}_{k+l|k}$ is also dependent on the probabilities of the measurement packets being successfully received by the base station. At time k, the information gain from A_i can be defined as

$$I_{i,k} = \chi_{i,k} \cdot H_{i,k}^{\mathrm{T}} R_{i,k}^{-1} H_{i,k} \tag{28}$$

where $\chi_{i,k} \sim \mathrm{Bern}(\beta_{i,k})$ is a random Bernoulli variable (either 0 or 1). $\beta_{i,k}$, which is determined by the packet-erasure channel model, indicates the probability of the packet successfully getting through from A_i to the base station. If the measurement packet from A_i is dropped by the base station, the information gain from A_i is $I_{i,k} = \mathbf{0}$. If the measurement packet can be transmitted from A_i to the base station successfully, the information gain from A_i is $I_{i,k} = H_{i,k}^{\mathrm{T}} R_{i,k}^{-1} H_{i,k}$.

For planning purposes, we need the value of the information gain in the future times $(k + l)$, thus the expectation must be used. At future times $(k + l)$, the prediction of the information gain matrix $\hat{I}_{k+l|k}$ is defined as

$$\hat{I}_{k+l|k} = \sum_{i=1}^{N} \beta_{i,k+l} \cdot \hat{H}_{i,k+l}^{\mathrm{T}} R_{i,k+l}^{-1} \hat{H}_{i,k+l} \tag{29}$$

$$\hat{H}_{i,k+l} = \nabla_{\hat{x}_{\mathrm{t},k+l|k}} h_i(x_{i,k+l|k}, \hat{x}_{\mathrm{t},k+l|k}) \tag{30}$$

In Equation (29), $x_{i,k+l|k}$ is the state of A_i at future time $(k + l)$, and which is defined as trajectory of A_i. $\hat{x}_{t,k+l|k}$ are the predictions of target state, which are computed as follows:

$$\hat{x}_{\mathrm{t},k+l|k} = f_{\mathrm{t}}(\hat{x}_{\mathrm{t},k+l-1|k}, \mathbf{0}) = F_{k+l-1} \hat{x}_{\mathrm{t},k+l-1|k} \tag{31}$$

In general, maximizing the FIM involves maximizing a matrix, which is difficult. Thus, it is necessary to find a scalar function based on the FIM to serve as an objective function in the observer trajectory optimization problem. Three common choices for scalar functions are the determinant (D-optimality criterion), the trace (A-optimality criterion), and the maximum eigenvalue (E-optimality criterion) of the FIM [14]. In this paper, the trace of the FIM, which is equal to the sum of its eigenvalues, was chosen as the desired scalar function. The eigenvalues of the FIM are related to the uncertainty hyper-ellipsoid of the target estimation, which depicts the distribution of the estimate error. More specifically, the sizes of the semi-axes of this hyper-ellipsoid are given by the reciprocal square of the eigenvalues. Therefore, maximizing the trace of the FIM leads to a smaller uncertainty hyper-ellipsoid; a more accurate estimation.

Thus, from Equations (27) and (29), the observer trajectory quality metric is defined as:

$$J_{k+l} = \mathrm{tr} \left(\left(F_{k+l-1} \hat{Y}_{k+l-1|k}^{-1} F_{k+l-1}^{\mathrm{T}} + G_{k+l-1} Q_{k+l-1} G_{k+l-1}^{\mathrm{T}} \right)^{-1} + \sum_{i=1}^{N} \beta_{i,k+l} \cdot \hat{H}_{i,k+l}^{\mathrm{T}} R_{i,k+l}^{-1} \hat{H}_{i,k+l} \right) \tag{32}$$

According to Equation (32), the observer-trajectory quality metric combines the sensing and communication channels into a utility function. This quantity metric is used to optimize the trajectories of the UAVs, so that the UAVs intelligently move to the locations that maximize both the information gains and the successful transmission probabilities in communication links with the base station.

4. Motion Planning Algorithm Based on Co-Optimization of Communication and Sensing

If the exact position and velocity of the target are known, optimal observer trajectories can be accurately designed. However, the target state is not known in advance, so the trajectory generator must continually re-plan the trajectory based on the results of the target state estimation. Hence, the multiple UAV cooperative target tracking problem is a real-time dynamic optimization problem. We use the combined communication and sensing utility function to plan optimal trajectories for the UAVs in the framework of receding horizon optimization.

4.1. Receding Horizon Optimizing Model for Multi-UAVs Cooperative Target Tracking

The receding horizon optimization model for multiple UAV cooperative target tracking at time k is:

$$\boldsymbol{u}^*[k+1:k+T_\mathrm{P}] = \arg\max_{u}\left\{\sum_{l=1}^{T_\mathrm{P}}(\lambda_{k+l}J_{k+l})\right\} = \arg\max_{u}\left\{\sum_{l=1}^{T_\mathrm{P}}\lambda_{k+l}\cdot\mathrm{tr}\left(\hat{\boldsymbol{Y}}_{k+l|k}\right)\right\} \tag{33}$$

subject to

$$\boldsymbol{x}_\mathrm{t}(k+1) = \boldsymbol{f}_\mathrm{t}(\boldsymbol{x}_\mathrm{t}(k),\boldsymbol{w}(k)) \tag{34}$$

$$\boldsymbol{x}_i(k+1) = \boldsymbol{f}_\mathrm{u}(\boldsymbol{x}_i(k),\boldsymbol{u}_i(k)) \tag{35}$$

$$\boldsymbol{z}_i(k) = \boldsymbol{h}_i(k,\boldsymbol{x}_i(k),\boldsymbol{x}_\mathrm{t}(k)) + \boldsymbol{v}_i(k) \tag{36}$$

$$\sqrt{(x_i-x_j)^2 + (y_i-y_j)^2} \geq d_\mathrm{safe}, i \neq j \tag{37}$$

where $\boldsymbol{u}[k+1:k+T_\mathrm{P}] = \{\boldsymbol{u}_1[k+1:k+T_\mathrm{P}], \boldsymbol{u}_2[k+1:k+T_\mathrm{P}], \ldots, \boldsymbol{u}_N[k+1:k+T_\mathrm{P}]\}$ denotes the vector of control inputs to all the UAVs over the time horizon $[k+1:k+T_\mathrm{P}]$. According to the UAV dynamic model, which is described by Equation (1), the control input $\boldsymbol{u}$ is the desired horizontal flight path angle (χ^c) of the aircraft. In this receding horizon optimization model, the purpose is to maximize the weighted sum of the trace of $\hat{\boldsymbol{Y}}_{k+l|k}$ over the time horizon $[k+1:k+T_\mathrm{P}]$, and $l = 1, 2, \ldots, T_\mathrm{P}$. The weight factors are given by $\lambda(k+l)$. Equations (34)–(36) denote the target dynamical model, the UAV dynamical model, and the sensor model, respectively. Equation (37) ensures collision avoidance between the UAVs, where d_safe is the safety distance for collision avoidance.

For maximizing the weighting sum of the trace of $\hat{\boldsymbol{Y}}_{k+l|k}$ over the time horizon $[k+1:k+T_\mathrm{P}]$, an approximate solution is to maximize the trace of $\hat{\boldsymbol{Y}}_{k+l|k}$ at time $(k+l)$. Thus, Equation (33) becomes

$$\boldsymbol{u}^*(k+l) = \arg\max_{u(k+l)}\{J_{k+l}\} = \arg\max_{u(k+l)}\left\{\mathrm{tr}\left(\hat{\boldsymbol{Y}}_{k+l|k}\right)\right\} \tag{38}$$

$$\hat{\boldsymbol{Y}}_{k+l|k} = \underbrace{\left(\boldsymbol{F}_{k+l-1}\hat{\boldsymbol{Y}}_{k+l-1|k}^{-1}\boldsymbol{F}_{k+l-1}^\mathrm{T} + \boldsymbol{G}_{k+l-1}\boldsymbol{Q}_{k+l-1}\boldsymbol{G}_{k+l-1}^\mathrm{T}\right)^{-1}}_{\hat{\boldsymbol{Y}}_{k+l|k}^-} + \underbrace{\sum_{i=1}^{N}\beta_{i,k+l}\cdot\hat{\boldsymbol{H}}_{i,k+l}^\mathrm{T}\boldsymbol{R}_{i,k+l}^{-1}\hat{\boldsymbol{H}}_{i,k+l}}_{\hat{\boldsymbol{I}}_{k+l|k}} \tag{39}$$

It can be seen from Equation (38) that we need to compute $\boldsymbol{u}^*(k+l) = \{\psi_1{}^*(k+l), \psi_2{}^*(k+l), \ldots, \psi_N{}^*(k+l)\}$, which are the control inputs for all of the UAVs at time $(k+l)$ in order to maximize the trace of $\hat{\boldsymbol{Y}}_{k+l|k}$ at time $(k+l)$. From Equation (39), the information matrix $\hat{\boldsymbol{Y}}_{k+l|k}$ is determined by a sum of two terms $\hat{\boldsymbol{Y}}_{k+l|k}^-$ and $\hat{\boldsymbol{I}}_{k+l|k}$. The first term in Equation (39), $\hat{\boldsymbol{Y}}_{k+l|k}^-$, represents the prediction of prior information obtained by propagating the corresponding EIF one step ahead, which is independent of the measurement results. The second term in Equation (39), $\hat{\boldsymbol{I}}_{k+l|k}$ represents the information gain

contained in the measurements of all the UAVs. $\hat{Y}_{k+l|k}^-$ is not related to $\boldsymbol{u}^*(k+l)$, so $\hat{Y}_{k+l|k}^-$ can be ignored, and the objective function J_{k+l} in Equation (38) can be reduced to:

$$
\begin{aligned}
\widetilde{J}_{k+l} &= \mathrm{tr}(\sum_{i=1}^{N} \beta_{i,k+l} \cdot \hat{\boldsymbol{H}}_{i,k+l}^{\mathrm{T}} \boldsymbol{R}_{i,k+l}^{-1} \hat{\boldsymbol{H}}_{i,k+l}) = \sum_{i=1}^{N} \left[\beta_{i,k+l} \cdot \mathrm{tr}(\hat{\boldsymbol{H}}_{i,k+l}^{\mathrm{T}} \boldsymbol{R}_{i,k+l}^{-1} \hat{\boldsymbol{H}}_{i,k+l}) \right] \\
&\leq \underbrace{\left(\sum_{i=1}^{N} \beta_{i,k+l} \right)}_{J_{k+l}^{\mathrm{commnication}}} \cdot \underbrace{\left(\sum_{i=1}^{N} \mathrm{tr}(\hat{\boldsymbol{H}}_{i,k+l}^{\mathrm{T}} \boldsymbol{R}_{i,k+l}^{-1} \hat{\boldsymbol{H}}_{i,k+l}) \right)}_{J_{k+l}^{\mathrm{sensing}}}
\end{aligned}
\tag{40}
$$

In Equation (40), the objective function $\widetilde{J}_{k+l}$ contains communication optimization item $J_{k+l}^{\mathrm{commnnication}}$ and sensing optimization item $J_{k+l}^{\mathrm{sensing}}$. Therefore, the co-optimization of communication and sensing is reflected in the tradeoffs between communication reliability and sensing utility, aims to maximize the overall information gain delivered to the base station.

In the framework of distributed receding horizon optimization, as shown in Figure 3, at time k, each UAV A_i receives the planned control inputs $\overline{\boldsymbol{U}}_{-i}(k)$ and the trajectories $\overline{\boldsymbol{X}}_{-i}(k)$ from the other UAVs. Then A_i optimizes its control inputs $\overline{\boldsymbol{U}}_i(k)$ and plans its own trajectory $\overline{\boldsymbol{X}}_i(k)$ based on the estimates of the target state and the future state predictions of the other UAVs. A_i also can share the optimal control inputs $\overline{\boldsymbol{U}}_i(k)$ and the planned trajectory $\overline{\boldsymbol{X}}_i(k)$ with the other UAVs. Thus, the distribution optimization is performed in a specific order [25]. For example, A_n plans its trajectory based on the trajectories of the previous $(n-1)$ aircrafts ($A_1 \sim A_{n-1}$) and then sends its trajectory to aircraft A_{n+1}.
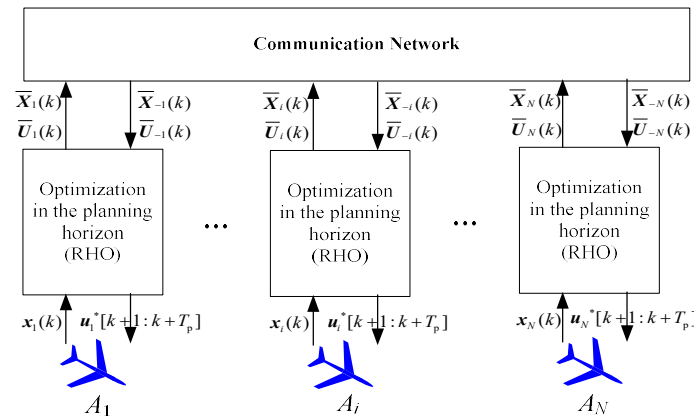

Figure 3. Sketch of the distributed decision-making model for multiple UAV cooperative target tracking.

UAV A_i computes its own trajectory by solving the following local optimization problem:

$$
\boldsymbol{u}_i^*[k+1:k+T_{\mathrm{P}}] = \arg \max_{u_i} \left\{ \sum_{l=1}^{T_{\mathrm{P}}} \lambda_{k+l} \cdot \mathrm{tr}\left(\beta_{i,k+l} \cdot \hat{\boldsymbol{H}}_{i,k+l}^{\mathrm{T}} \boldsymbol{R}_{i,k+l}^{-1} \hat{\boldsymbol{H}}_{i,k+l} \right) \right\}
\tag{41}
$$

with the constraints of Equations (34)–(36).

4.2. Communication Topology Optimization Based on a Minimum Weighted Spanning Tree

In this paper, the packet routing algorithm always chooses the route with the highest successful transmission probability. To find such a route, we define the weight of each link as:

$$
W^{m,n} = -\ln(P_r^{m,n})
\tag{42}
$$

where smaller weight, indicates a higher the probability of successful transmission. For UAV A_i, the problem of finding the route with the highest successful transmission probability can be represented via solving:

$$\text{route}^*_{i,k} = \arg\max_{\text{route}_{i,k}} \beta_{i,k} = \arg\min_{\text{route}_{i,k}} \left[\sum_{(m,n)\in\text{route}_{i,k}} W^{m,n} \right] \tag{43}$$

which can be solved by Dijkstra algorithm.

For the entire multiple UAV system, to ensure that all the UAVs and the base station relate to the highest successful transmission probabilities, the concept of the minimum weighted spanning tree (MST) [26] from graph theory is used to determine the topology of the communication network. Figure 4 shows an example communication topology and its minimum weighted spanning tree. The base station is the root node that directly or indirectly connects to all the other nodes (the UAVs). The MST must connect all nodes with the condition that the sum of the weights is minimized. Thus, the overall probability of a message "floating" in the MST network is maximized.
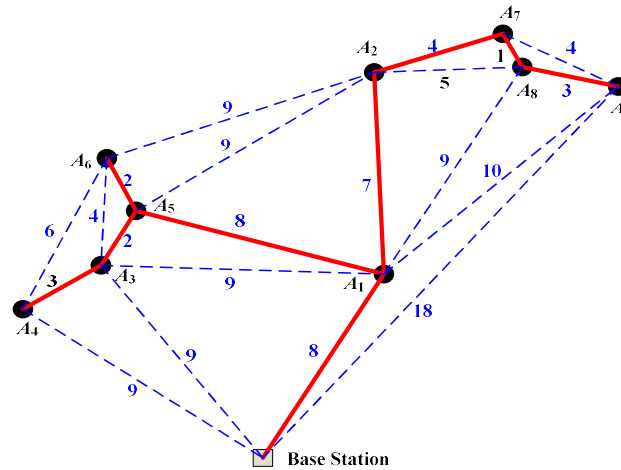
Figure 4. Example of a communication topology and its corresponding minimum weighted spanning tree.

At each time k, the MST can be constructed according to the positions of UAVs and the base station. Based on such MST communication topology, Dijkstra algorithm is used to find the route with the highest successful transmission probability between each UAV A_i and the base station. The MST communication topology determines the planning hierarchy, which is the order of the optimization calculation in the distributed frame. All UAVs are sorted in the ascending order of their total hops numbers of the optimal transmission route to the base station. If the total hops are the same, they are arranged in ascending order of their identity numbers. This sorted result is the planning hierarchy, in which each UAV plans its trajectory based on the planned results of the aircrafts which are higher in the hierarchy and sent the planned results to the aircrafts which are lower in the hierarchy. For example, in Figure 4, A_1 acts a relay for A_2, thus the successful transmission probability between A_2 and the base station can be represented as $\beta_{2,k+l} = \beta_{2\rightarrow 1,k+l} \cdot \beta_{1,k+l}$. Where $\beta_{1,k+l}$ denotes the transmission probability between A_1 and the base station, and $\beta_{2\rightarrow 1,k+l}$ denotes the transmission probability between A_2 and A_1. It can be seen that A_1 computes its own trajectory by itself, while A_2 computes the trajectory based on the planned results of A_1.

4.3. Cooperative Target Tracking Algorithm Based on Co-Optimization of Communication and Sensing

The block diagram in Figure 5 summarizes the cooperative target tracking algorithm based on the co-optimization of communication and sensing. At each time k, first, according the positions of UAVs and the base station, the weighted minimum spanning tree strategy is used to optimize the communication network topology. Based on the MST communication topology, the Dijkstra algorithm

is used to find the route with the highest successful transmission probability between each UAV A_i and the base station. Next, all the UAVs are sorted in the ascending order of the total number of hops to the base station as described in the previous section. The UAVs successively perform the local optimization calculation according to the sorted results. Next, each UAV A_i uses an EIF to obtain the local estimation results $\hat{x}_{t,i,k|k}$ of the target state. The local information terms $i_{i,k}$ and $I_{i,k}$, which are generated based on the measurement $z_{i,k}$ of the target, are summed at the base station to produce a global estimation. A_i then computes its own trajectory based on the planned results of A_j, which is the relay of A_i in the current MST communication topology. In distributed fashion, each UAV A_i solves the local optimization problem in Equation (42) to obtain the optimal control sequence $u^*_{i,k}$ during a planning time horizon T_P. Finally, the control input in the sequence is implemented, A_i changes its flight state $x_{i,k}$, and obtains a new measurement $z_{i,k}$ of the target restarting the cycle.
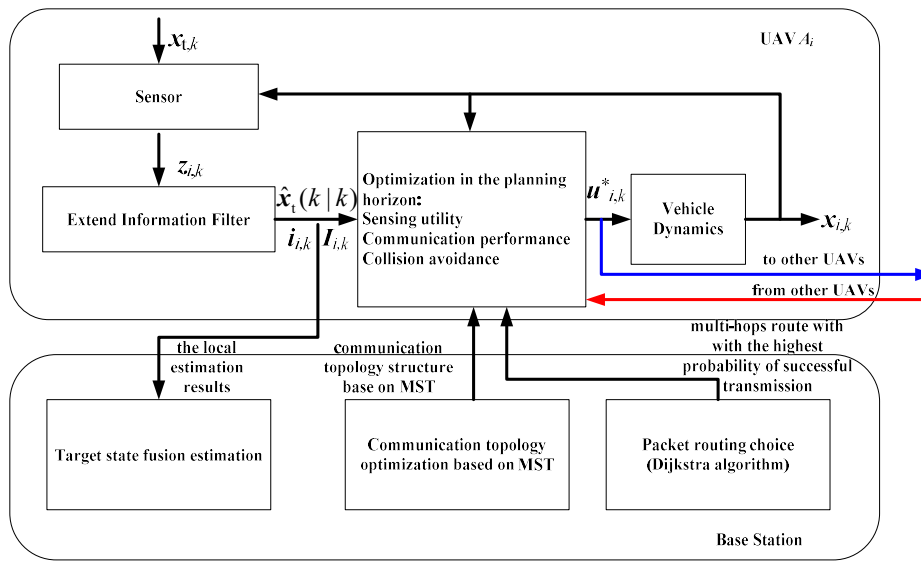
Figure 5. Processing diagram for multi-UAVs cooperative target tracking algorithm.

Remark 2. *Our algorithm uses the concept of the MST to optimize the communication network topology according to the positions of the UAVs and the base station. The MST communication topology determines the planning hierarchy, which determines the order of the optimization calculation in the distributed framework. In this way, our algorithm can effectively adapt to a dynamic environment such as moving targets and the non-static spatial distribution of the UAVs. Thus, in the dynamic scenario of tracking a moving target, our algorithm can produce a more efficient target state estimate than the algorithm in Reference [18]. However, there is a limitation in our algorithm, which also exists in Reference [18]; the scalability of the planning approach. As trajectory optimization is performed sequentially, each UAV plans its own trajectory based on the planned results of other UAVs. For large networks, exchanging the planned trajectories between the UAVs requires many communications. However, due to the bandwidth limitation of realistic wireless communication links, it is hard to receive all the required information within one sampling time. In addition, as the number of UAVs increases, solving the optimization problem in Equation (42) becomes difficult in real time. In future work, we will design a planning algorithm with low computational complexity.*

5. The Simulation Validation and Results Analysis

5.1. Comparative Simulations for Communication Optimization

In Scenario 1, a single moving target T is continuously tracked by two UAVs, A_1 and A_2. The detailed initial settings of the UAVs are listed in Table 2. The ground speed of the UAVs is

v_i = 50 m/s, and their maximum turning rate is ω_{max} = 30 deg/s. The target motion is modeled by Equation (4), its initial position is $(-800, 0)$ m, its initial movement direction is -20 deg, and its noise is characterized by $\delta_x = \delta_y = 0.1$ m/s^2. The standard deviations in the sensor model are $\delta_r = 2$ m and $\delta_\theta = 0.05$ rad. The position of the base station B is $(-500, -800)$ m. The communication model is shown in Figure 2 and the relevant parameters in Table 1. The simulating time of each simulation is 100 s, with a time step of $T_s = 1$ s. Finally, the planning time horizon is set at $T_P = 3$ s and the safety distance for collision avoidance is $d_{safe} = 100$ m.

Table 2. The initial settings of two UAVs in Scenario 1.

UAV A_i	Position (x_i, y_i)/(m)	Heading Angle Ψ_i/(°)
A_1	$(-400, -700)$	45
A_2	$(-800, 200)$	0

To verify the effectiveness of cooperative target tracking algorithm based on co-optimization of communication and sensing, the two groups of experiments are carried out.

- Group A: with communication optimization; and
- Group B: without communication optimization.

5.1.1. Group A: With Communication Optimization

Figures 6–8 show the trajectories at 30 s, 64 s, and 100 s, respectively. In these figures, the communication links are denoted by cyan thin dashed lines. The numbers represent the successful transmission probabilities of the links. The arrows denote the movement directions of the UAVs. It can be seen from Figure 6, that at the beginning of the simulation ($t = 30$ s), A_1 is closer to the base station and A_2 is farther away from the base station, thus A_1 orbits near the base station to act as a relay for maintaining connectivity between A_2 and the base station B. At this time, A_2 is tracking target T, and sending its local estimation results back to base station B through the relay A_1. With the movement of the target, the distance between the target T and the base station B gradually is reduced. Since A_1 is orbiting near the base station, the distance between T and A_1 also gradually is decreased causing A_1 to gradually move up and track the target T. When $t = 64$ s, as shown in Figure 7, the topology of the communication network is changed and A_2 acts as a relay for A_1. As the target moves away from the base station, for example at $t = 100$ s as shown in Figure 8, A_2 moves near the base station to continuously act as the relay for A_1, and A_1 orbits near the target T to track it.
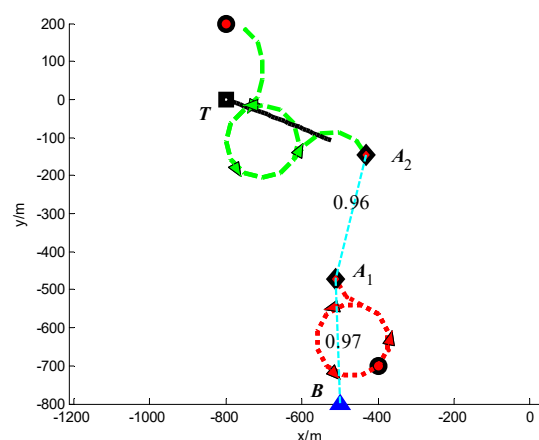
Figure 6. Trajectories of UAVs and target at $t = 30$ s (Group A in Scenario 1).
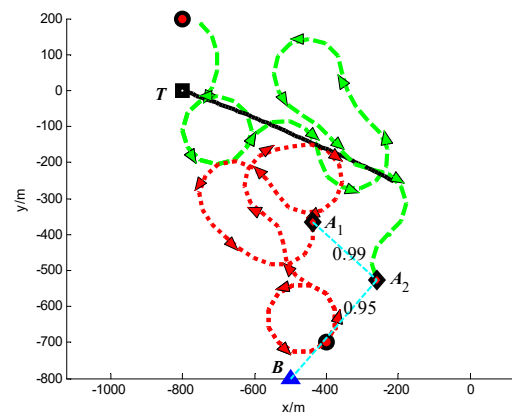
Figure 7. Trajectories of UAVs and target at *t* = 64 s (Group A in Scenario 1).
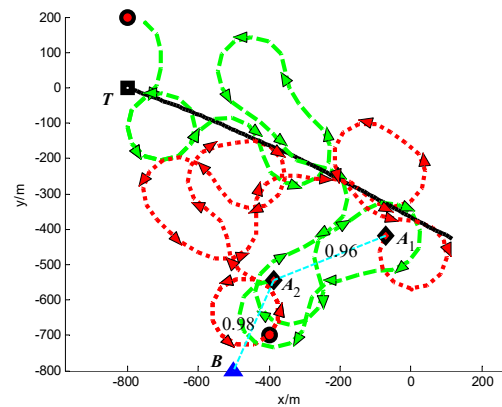

Figure 8. Trajectories of UAVs and target at *t* = 100 s (Group A in Scenario 1).

Figure 9 shows that the successful transmission probabilities of A_1 and A_2. It can be seen that A_1 acts as the relay for A_2 during the time period [0, 64) s, and A_2 acts as the relay for A_1 during the time period [64, 100] s. In addition, it can be seen that, when communication optimization is considered, the average transmission probabilities of A_1 and A_2 to base station are 0.9076 and 0.8504, respectively. However, if A_1 and A_2 communicate with the base station directly without any relay, their average transmission probabilities are 0.8627 and 0.7730, respectively. Thus, the communication performances of A_1 and A_2 are improved by our algorithm with considering the communication optimization.
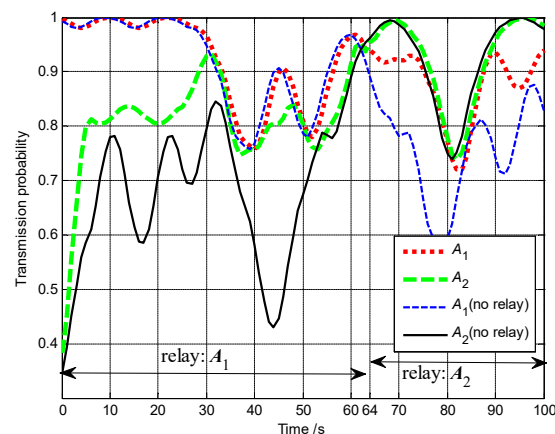
Figure 9. The probabilities of successful transmission of A_1 and A_2 to base station (Group A in Scenario 1).

The track of the FIM of A_1, A_2 and base station is shown in Figure 10. Due to considering communication optimization, the probabilities of a successful transmission of A_1 and A_2 to the base station are almost larger than 0.7 in Group A. Thus, A_1 and A_2 can transmit their measurement packets back to the base station, which can significantly enhance the global estimate performance and then improve the effectiveness of multi-UAVs cooperative target tracking.
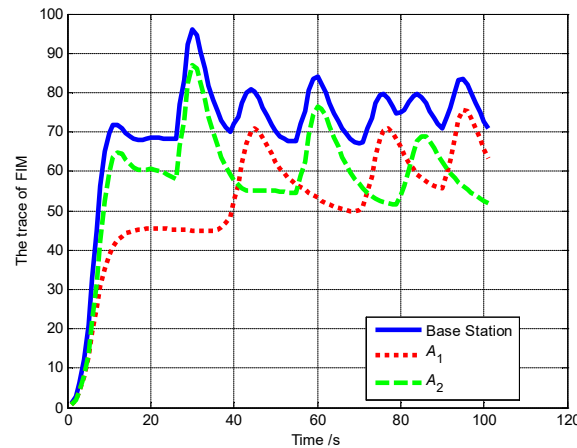
Figure 10. The track of FIM of A_1, A_2 and base station (Group A in Scenario 1).

Figure 11 shows the distance between A_1, A_2. The distance is always larger than the safety distance (d_{safe} = 100 m), thus the safety of the UAVs is guaranteed.
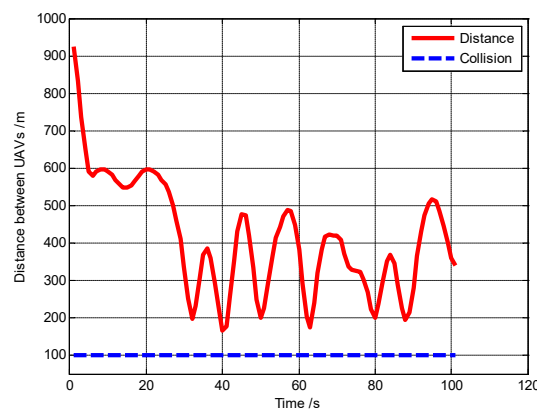

Figure 11. The distance between the UAVs during the simulation process (Group A in Scenario 1).

5.1.2. Group B: Without Communication Optimization

Figures 12–14 show the trajectories at 30 s, 64 s and 100 s, respectively for UAVs without communication optimization. The algorithm without communication optimization only focus on sensing optimization item $J_{k+l}^{sensing}$, and thus guides both A_1 and A_2 toward the target to maximize the information gain. However, with A_1 and A_2 flying away from the base station, a significant amount of measurement packets is dropped by the base station. This conclusion is confirmed in Figure 15. As shown in Figure 15, in Group B, the average transmission probabilities of A_1 and A_2 are only 0.6717 and 0.6276, respectively. It means that, in Group B, there are more packets from A_1 and A_2 are dropped (not received) by the base station than in Group A. The measurements contained in the dropped packets will not be incorporated into the global estimate result of the target state. As shown in Figure 16, the track of the FIM at the base station shows zero growth and a small downtrend over a long time (20 s~100 s). Figure 17 shows the distance between A_1, A_2. The distance is always larger than the safety distance (d_{safe} = 100 m), and thus the safety of the UAVs is guaranteed.
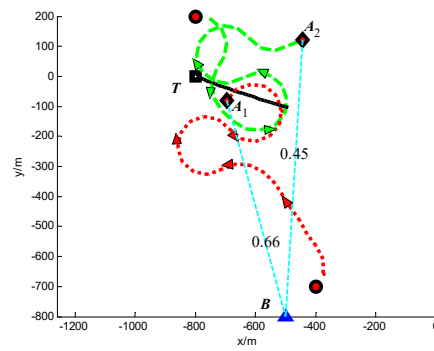
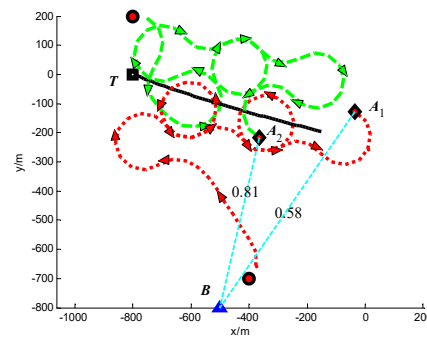**Figure 12.** Trajectories of UAVs and target at *t* = 30 s (Group B in Scenario 1).

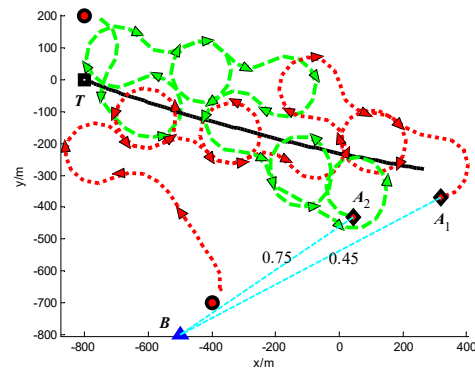**Figure 13.** Trajectories of UAVs and target at *t* = 64 s (Group B in Scenario 1).

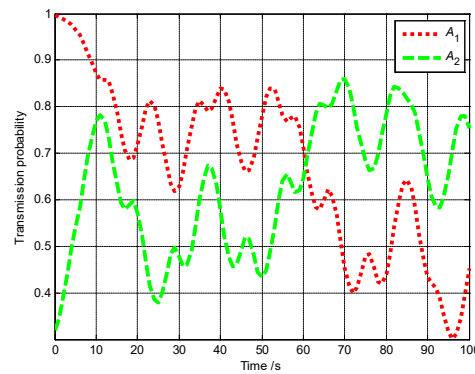**Figure 14.** Trajectories of UAVs and target at *t* = 100 s (Group B in Scenario 1).

Figure 15. The probabilities of successful transmission of A_1 and A_2 to base station (Group B in Scenario 1).
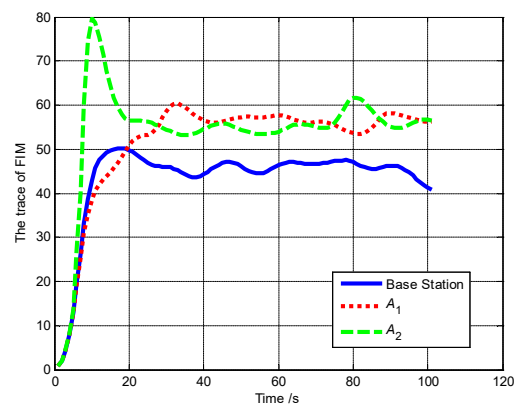
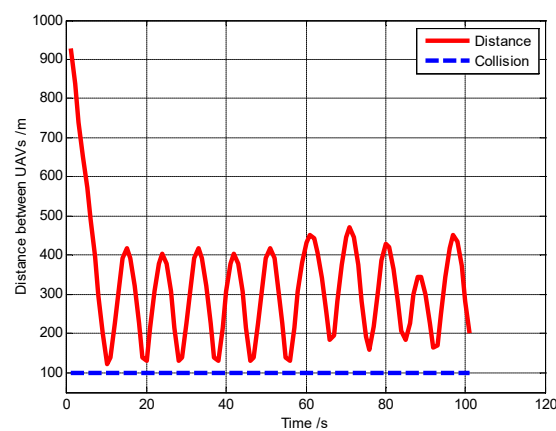**Figure 16.** The trace of the FIM for A_1, A_2 and base station (Group B in Scenario 1).

Figure 17. The distance between the UAVs during the simulation process (Group B in Scenario 1).

5.1.3. Monte-Carlo Simulations for Scenario 1

Due to the acceleration noise in the target model and the measurement noise in the sensor model, the results of a single simulation are not sufficient to illustrate that the proposed method is effective. Hence, we run ten times Monte-Carlo simulations for Scenario 1 to further analyze the performance of the target state estimation in two cases. The statistical results—such as the average errors of the target state estimation (position, speed, movement direction)—the average transmission probabilities, the average trace of the FIM, are shown in Table 3.

Table 3. Comparison of the average estimate errors, the average transmission probabilities, and the average trace of the FIM in Scenario 1 (Group A vs. Group B).

Item	Group	Base Station	A_1	A_2
Average estimation error for position (m)	A	1.2778	3.4806	1.9570
	B	1.6287	2.4619	1.9565
Average estimation error for speed (m/s)	A	0.2100	0.3110	0.2714
	B	0.2451	0.2931	0.2493
Average estimation error for direction (°)	A	1.2098	1.5951	1.3775
	B	1.2133	1.5253	1.3121
Average transmission probability	A	-	0.8858	0.8056
	B	-	0.7359	0.6203
Average trace of the FIM	A	72.4468	50.5545	55.9077
	B	46.2311	52.0081	60.4408

- For the base station, the average errors in the estimation of the target state (position, speed, movement direction) in Group A are less than in Group B, and the average trace of the FIM in Group A is larger than in Group B. Thus, when communication optimization is considered, the global estimate results for the target state are more accurate and more effective. This is because our algorithm maximizes the information gain while considering communication reliability. The remote UAVs can successfully transmit their measurement packets back to the base station with other UAVs acting as communication relays. These measurements are used to improve the accuracy and effectiveness of the global estimate results.

- For A_1 and A_2, their target state estimate results in Group B are better than in Group A in terms of the average errors and the average trace of the FIM. The reason is that, in Group B, the algorithm only focuses on sensing optimization, and guides both A_1 and A_2 toward the target to maximize the information gain. However, A_1 and A_2 are outside the range for direct communication to the base station, and then the measurements obtained from A_1 and A_2 do not contribute to the global estimate results of the target state.

- In Group A, A_2 has lower average estimate errors and larger the average trace of the FIM than A_1. It implies that A_2 has better sensing performance than A_1. This is because A_1 acts as a relay for A_2 in a long time. To establish a multi-hops chain to get the measurement packets from A_2 back to the base station, A_1 orbits near the base station, and hence cannot get better sensing information from the target. These results illustrate how the proposed algorithm implements tradeoffs between communication performance and sensing utility.

5.2. The Effect of Different Communication Topology Optimization Strategies

As mentioned above, the planning hierarchy of the UAVs is determined by the communication topology structure. In the proposed approach, the communication topology structure is optimized by the weighted minimum spanning tree strategy. However, in Reference [18], the planning hierarchy of the UAVs is determined according to the identity numbers of the UAVs. Since the identity numbers of the UAVs are pre-defined, the planning hierarchy is fixed. A Fixed planning hierarchy results in a fixed communication topology structure. More specifically, the UAVs automatically establish a fixed multi-hop chain, where the UAV A_i acts as relay for the UAV A_{i+1}. To analyze the effect of different communication topology optimization strategies on the performance of cooperative target tracking, the proposed method is compared with the method of Reference [18] by setting up the following two group experiments.

- Group A: the minimum spanning tree topology (the proposed method);
- Group B: fixed communication topology structure (the method of Reference [18])

In Scenario 2, two UAVs A_1 and A_2 locate a single static target T. The detailed initial settings of the UAVs are listed in Table 4. The position of the static target is $(-800, 0)$ m, and the position of the base station B is $(-500, -800)$ m. The other simulation conditions are identical to Scenario 1.

Table 4. The initial settings of the two UAVs in Scenario 2.

UAV A_i	Position (x_i, y_i)/(m)	Heading Angle Ψ_i/(°)
A_1	$(-800, 200)$	45
A_2	$(-400, -700)$	180

5.2.1. Group A: The Minimum Spanning Tree Topology

Figures 18 and 19 show the trajectories at 10 s and 100 s, respectively. The transmission probabilities of A_1 and A_2 to base station are shown in Figure 20. The trace of the FIM for A_1, A_2 and base station are shown in Figure 21. We can conclude that, due to A_2 being closer to the base station than A_1, the communication topology structure based on the weighted minimum spanning tree is $\{A_1 \rightarrow A_2 \rightarrow B\}$. With A_2 acting as the relay of A_1, A_2 should to make a tradeoff between

communication and sensing. Therefore, A_2 finds the optimal location $O_2 = (-520.4, -557.6)$ m, where the information gain and the probability of a successful transmission with the base station are both optimal. Due to the dynamic constraints, A_2 continue to orbit around the optimal position O_2. At the same time, A_1 continue to orbit around the target T.
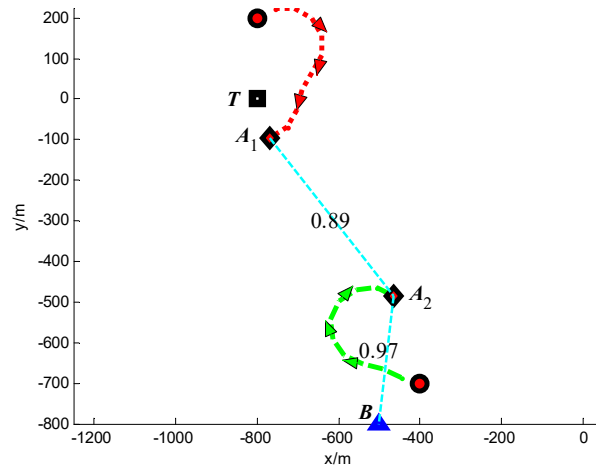
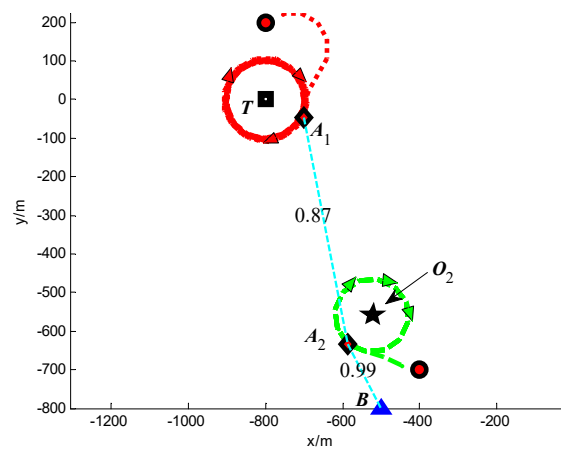**Figure 18.** Trajectories of UAVs at $t = 10$ s (Group A in Scenario 2).
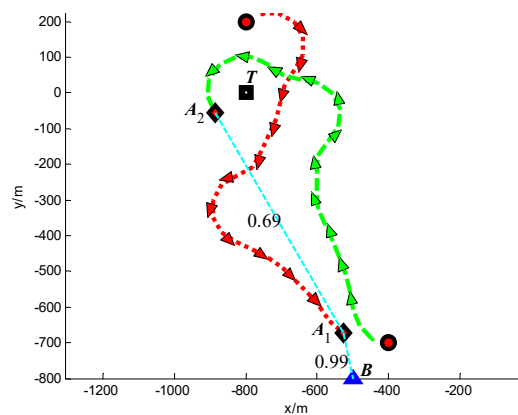
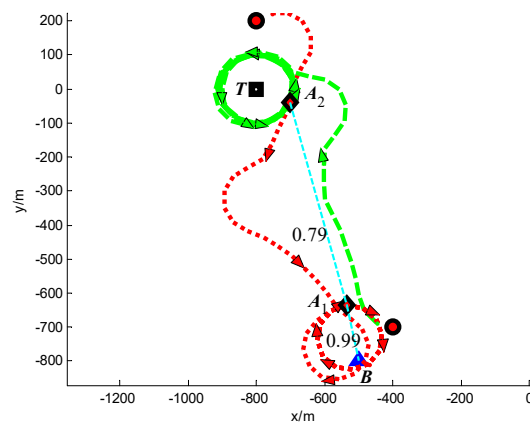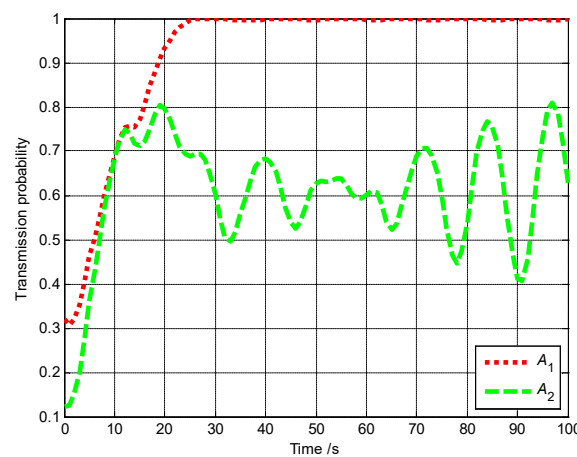**Figure 19.** Trajectories of UAVs at $t = 100$ s (Group A in Scenario 2).
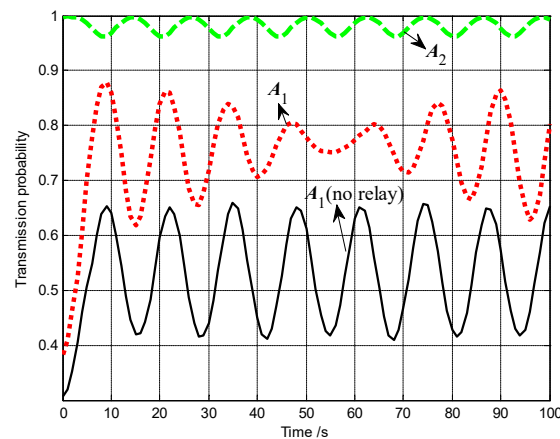
Figure 20. The probabilities of successful transmission of A_1 and A_2 to base station (Group A in Scenario 2).
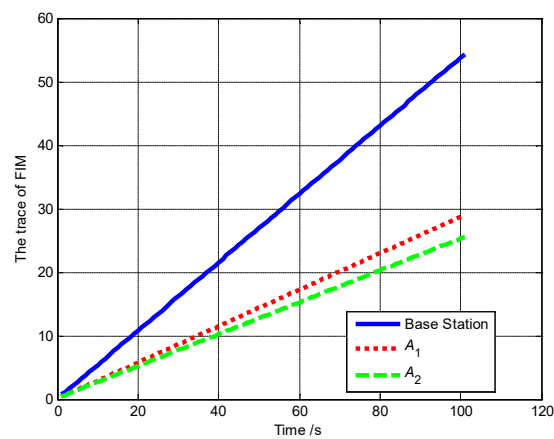
Figure 21. The trace of the FIM for A_1, A_2 and base station (Group A in Scenario 2).

5.2.2. Group B: Fixed Communication Topology Structure

Figures 22–24 show the trajectories at 10 s, 20 s and 100 s, respectively. In Group B, identical to Reference [18], the fixed communication topology structure is $\{A_2 \rightarrow A_1 \rightarrow B\}$. However, A_1 is initially closer to the target and A_2 is initially closer to the base station, so this fixed communication topology is not optimal obviously. To form and maintain this fixed topology, A_1 moves toward the base station while A_2 moves toward the target, as shown in Figure 22.
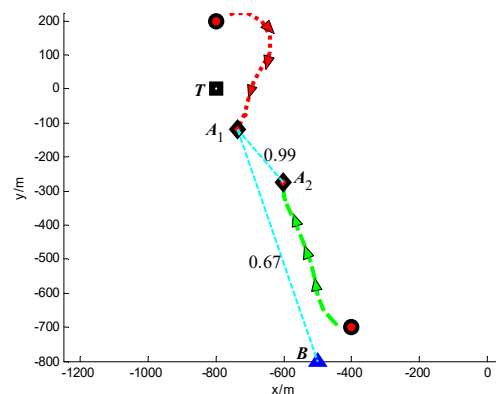
Figure 22. Trajectories of UAVs at t = 10 s (Group B in Scenario 2).

Figure 23. Trajectories of UAVs at t = 20 s (Group B in Scenario 2).

Figure 24. Trajectories of UAVs at $t = 100$ s (Group B in Scenario 2).

The pre-set fixed topology is unreasonable, which causes A_1 and A_2 to perform unnecessary maneuvers. It can be seen from Figure 25 that, the transmission probabilities of A_1 and A_2 to base station are low, which reduce the global estimate performance. This can be confirmed in Figure 26. During the period of [0, 20] s, the trace of FIM in the base station is less than A_1 and A_2. This is because the ground station failed to receive the measurement packets from A_1 and A_2.

Figure 25. The probabilities of successful transmission of A_1 and A_2 to base station (Group B in Scenario 2).
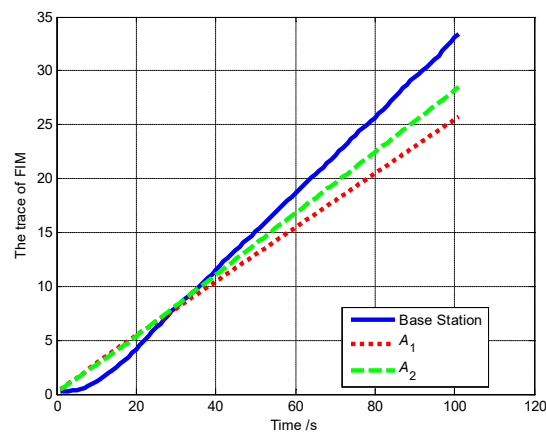
Figure 26. The track of the FIM for A_1, A_2 and base station (Group B in Scenario 2).

5.2.3. Monte-Carlo Simulations for Scenario 2

Again, we ran ten Monte Carlo simulations for Scenario 2. The statistical results are shown in Table 5.

Table 5. Comparison of the average estimate errors, the average transmission probabilities, and the average trace of the FIM in Scenario 2 (Group A vs. Group B).

Item	Group	Base Station	A_1	A_2
Average estimation error for position (m)	A	0.4266	0.7203	1.1680
	B	0.5081	0.9029	0.7240
Average transmission probability	A	-	0.7463	0.9818
	B	-	0.9209	0.6051
Average trace of the FIM	A	27.4777	14.6744	13.0033
	B	15.5617	13.1899	14.2413

It can be seen from Table 5 that, compared with the fixed communication topology strategy, the global estimate results are more accurate and more effective by using the topology optimization strategy. The simulation results verify the rationality and validity of the topology optimization strategy based on the minimum spanning tree.

5.3. Performance of the Algorithm in a Complex Scenario

The following experiments are presented to verify the performance of the algorithm in more complex scenarios.

5.3.1. Three UAVs Tracking One Moving Target

In Scenario 3, a moving target T is continuously tracked by three UAVs A_1, A_2 and A_3. The detailed initial settings of the UAVs are listed in Table 6. The initial position of target is $(-800, 600)$ m. The position of the base station B is $(-500, -1000)$ m. The safety distance for collision avoidance is $d_{\text{safe}} = 250$ m. The other simulation conditions are same with Scenario 1.

Table 6. The initial settings of three UAVs in Scenario 3.

UAV A_i	Position (x_i, y_i)/(m)	Heading Angle Ψ_i/(°)
A_1	$(-400, -900)$	10
A_2	$(-800, 300)$	0
A_3	$(-800, 0)$	0

The snapshots, Figures 27–29, show the trajectories and communication topology of the UAVs at 10 s, 50 s and 100 s, respectively. In the tracking process, the MST communication topology is $\{A_2 \rightarrow A_3 \rightarrow A_1 \rightarrow B\}$. With A_3 and A_1 acting as the relays, A_2 gets close to the target to get better measurements and then circles it around. A_1 automatically sets itself up as a relay for A_3, so it is close enough to the base station. A_3 takes advantage of the position of A_1 to fly closer to A_2 and acts as the relay for A_2. Although A_2 is too far from the base station, it still can send its measurements back to the base station successfully.

The communication performances of A_1, A_2 and A_3 are shown in Figure 30. The average transmission probability of A_2 can be improved to about 0.5. By contrast, if A_2 communicates with the base station directly without any relay, its average transmission probability is lower than 0.1. Thus, the communication performance of A_2 is vastly improved with A_3 and A_1 acting as the relays.
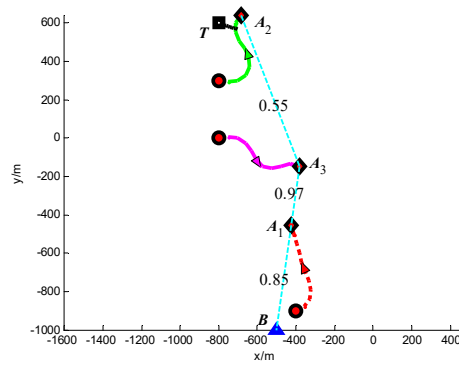
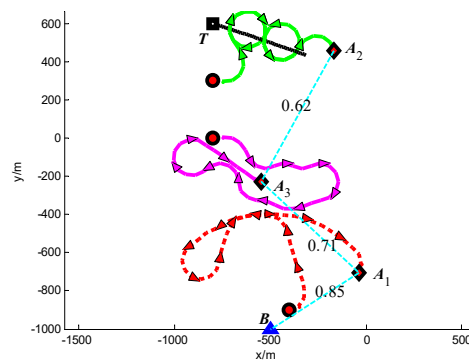**Figure 27.** Trajectories of UAVs and target at $t = 10$ s (Group A in Scenario 3).

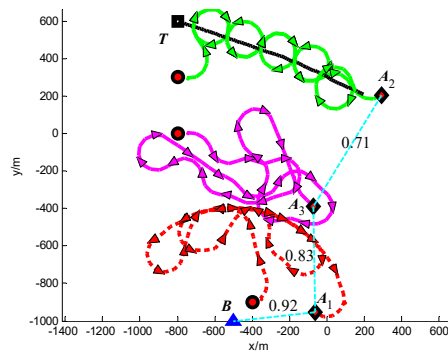**Figure 28.** Trajectories of UAVs and target at $t = 50$ s (Group A in Scenario 3).

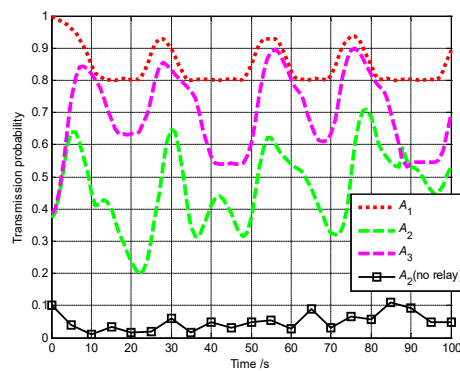**Figure 29.** Trajectories of UAVs and target at $t = 100$ s (Group A in Scenario 3).

Figure 30. The communication performances of A_1, A_2 and A_3 (Scenario 3).

The trace of the FIM is shown in Figure 31. To establish a reliable multi-hops chain between A_2 and the base station, A_3 and A_1 get close to the base station act as relays for A_2. Hence, A_3 and A_1 have no information gathering, and their trace of FIM have no change in the long time.
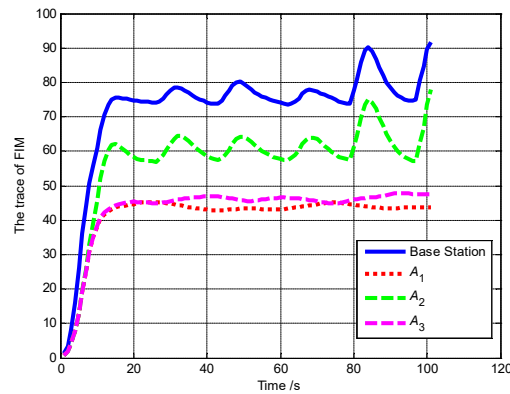

Figure 31. The track of FIM of A_1, A_2, A_3 and base station (Scenario 3).

Figure 32 shows that the safety of the UAVs is guaranteed because the minimum distance between UAVs is always larger than the safety distance ($d_{\text{safe}} = 250$ m).
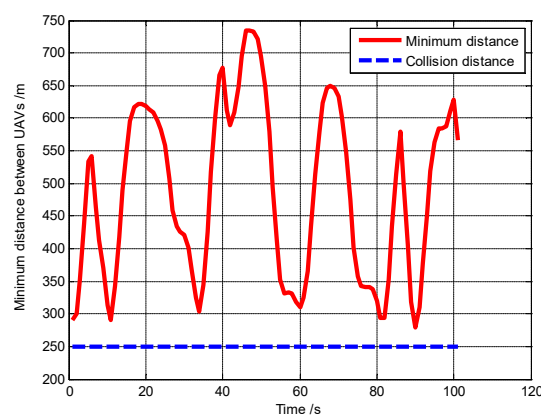

Figure 32. The minimum distance between the UAVs during the whole simulation process (Scenario 3).

In Scenario 3, the average estimate errors, the average transmission probabilities, the average trace of the FIM are shown in Table 7.

Table 7. The average estimate errors, the average transmission probability, and the average trace of the FIM in Scenario 3.

Item	Base Station	A_1	A_2	A_3
Average estimation error for position (m)	1.2454	6.2889	1.7638	4.0183
Average estimation error for speed (m/s)	0.2338	0.4282	0.2457	0.3552
Average estimation error for direction (°)	1.1365	1.1575	1.7017	1.4710
Average transmission probability	-	0.8485	0.4653	0.6953
Average trace of the FIM	72.4623	41.2674	57.2770	43.1731

It can be seen from Table 7 that, our algorithm integrates the communication and sensing objectives, so that the UAVs intelligently move to the locations that maximize both the information gained and the successful transmission probabilities in communication links with the base station. Thus, the base station can obtain a good estimate result of the target state.

5.3.2. Three UAVs Localizing One Static Target

In Scenario 4, a single moving target T is localized by three UAVs A_1, A_2 and A_3. The detailed initial settings of the UAVs are listed in Table 8. The position of the static target is $(-300, 600)$ m, and the position of the base station B is $(0, -200)$ m. The safety distance for collision avoidance $d_{safe} = 100$ m.

Table 8. The initial settings of three UAVs in Scenario 4.

UAV A_i	Position (x_i, y_i)/(m)	Heading Angle $\Psi_i/(°)$
A_1	$(100, -100)$	180
A_2	$(-100, 400)$	180
A_3	$(-300, 800)$	45

The snapshots, Figures 33 and 34 show the trajectories and communication topology of the whole UAVs at 10 s and 100 s, respectively. From these snapshots, we can see that, the UAVs automatically establish a multi-hops chain $\{A_3 \rightarrow A_2 \rightarrow A_1 \rightarrow B\}$. Due to A_1 being close enough to the base station, A_1 continue to orbit around the optimal position $O_1 = (-21.8, 44.3)$ m to re-transmit the measurement packets back to the base station. A_2 takes advantage of the position of A_1 to acts as the relay for A_3. The optimal position of A_2 is $O_2 = (-96.1, 306.8)$ m. A_3 gets close to the target from its starting position and keeps orbiting around the target T for better observation.
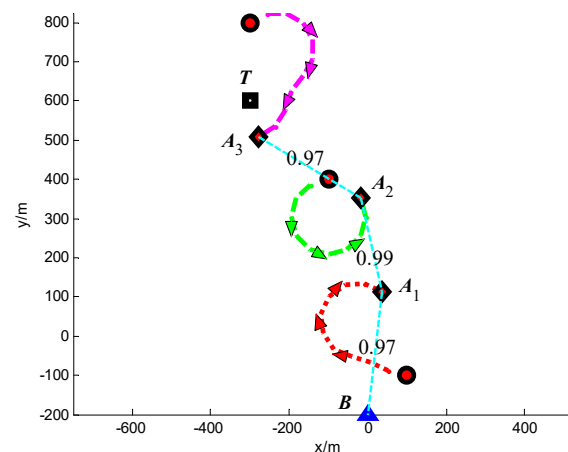

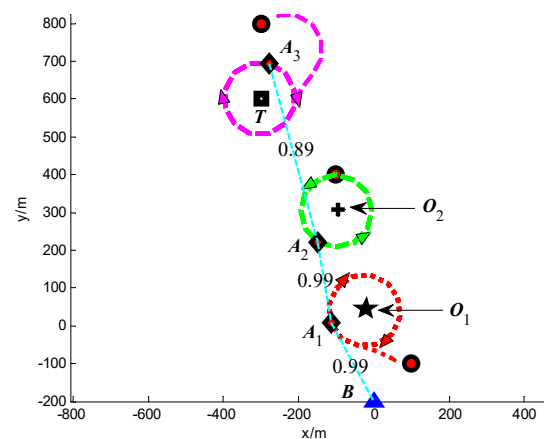
Figure 33. Trajectories of UAVs at $t = 10$ s (Scenario 4).

Figure 34. Trajectories of UAVs at $t = 100$ s (Scenario 4).

The communication performances of A_1, A_2 and A_3 are shown in Figure 35. The average transmission probability of A_3 is 0.8894. In contrast, if A_3 directly communicates with the base station without any relay, its average transmission probability is only 0.5215. The communication performance of A_3 is vastly improved with A_1 and A_2 acting as the relays.
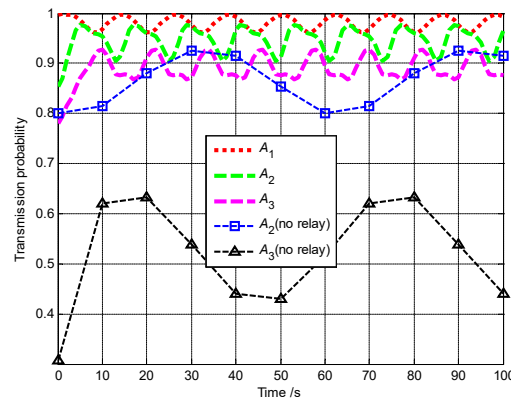

Figure 35. The communication performances of A_1, A_2 and A_3 (Scenario 4).

The trace of the FIM of A_1, A_2 A_3 and base station is shown in Figure 36 during the whole simulation process. A_2 gets close to the target to get better measurements and send its measurements back to the base station by the multi-hops chain $\{A_3 \rightarrow A_2 \rightarrow A_1 \rightarrow B\}$. Hence, the base station has good estimation performance.
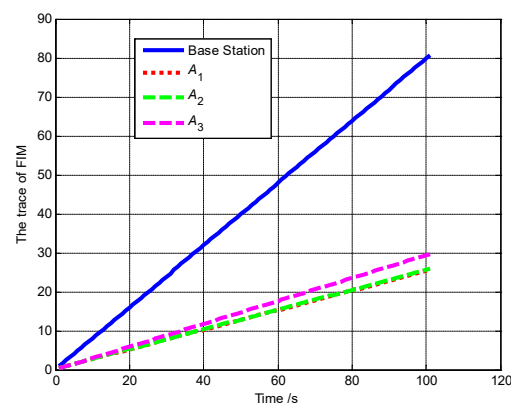

Figure 36. The trace of FIM of A_1, A_2, A_3 and base station (Scenario 4).

In Scenario 4, the average estimate error of the target position, the average transmission probabilities, the average trace of the FIM are shown in Table 9.

Table 9. The average estimate errors, the average transmission probability, and the average trace of the FIM in Scenario 4.

Item	Base Station	A_1	A_2	A_3
Average estimation error for position (m)	0.4535	1.2332	0.8105	0.4610
Average transmission probability	-	0.9818	0.9460	0.8894
Average trace of the FIM	40.7112	13.0033	13.1245	14.9834

It can be seen from Table 9 that, our algorithm can make UAVs more focus on maintaining good communication with base station or other UAVs in the mission process, so as to improve the performance of the target position estimation.

5.4. Effect of Varying Number of UAVs on Estimation Performance

In Scenario 5, we test the performance of the global estimation of the target state on the number of deployed UAVs. Using Monte Carlo simulations, we tested cases where the number of UAVs ranged from $N = 2$–10. For each case 100 independent experiments were performed. For each experiment, the initial positions and the initial heading angles of the UAVs, and the initial positions of targets are randomly generated in a 2 km × 2 km bound region. The ground speed of the UAVs is $v_i = 50$ m/s, the maximum turning rate of the UAVs is $\omega_{max} = 30$ deg/s. For the target, its initial position is $(-1000, 1000)$ m, and its initial movement direction is -20 deg. The position of the base station B is $(0, -1000)$ m. The safety distance for collision avoidance is $d_{safe} = 200$ m. The other simulation conditions are the same as Scenario 1.

The average estimate errors of target position, speed and direction are shown in Figures 37–39, respectively. The average trace of FIM is shown in Figure 40. From Figures 37–39, we can summarize that, the larger number of UAVs, the smaller average estimation errors. It implies the global estimation results are more accurate with increasing the number of the UAVs. From Figure 40, we can conclude that, the larger number of UAVs, the higher average trace of FIM. It implies the global estimate results are more effective with increasing the number of the UAVs. Therefore, the performance of the global estimate of target state will be improved as the number of the UAVs increases. This is for two reasons. On one hand, more UAVs implies more information obtained at each time step, which is beneficial for improving the global estimation performance. On the other hand, with increasing the number of UAVs, the operational range of the UAV swarm can be extended, due to more UAVs being used as relays to provide measurement packets to the remote station. In this case, several UAVs can get close to the target for better observations while their measurement packets can be sent back to base station successfully. It is also beneficial for improving the global estimation performance.
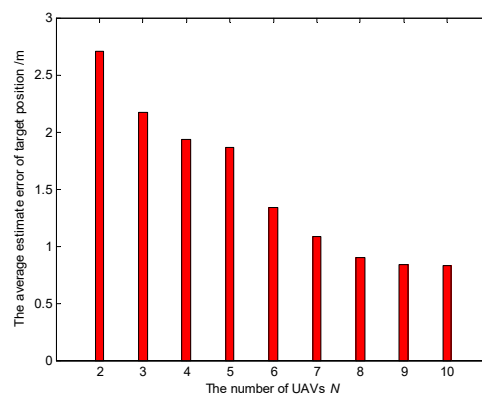

Figure 37. The average estimation error of target position for different numbers of UAVs (Scenario 5).
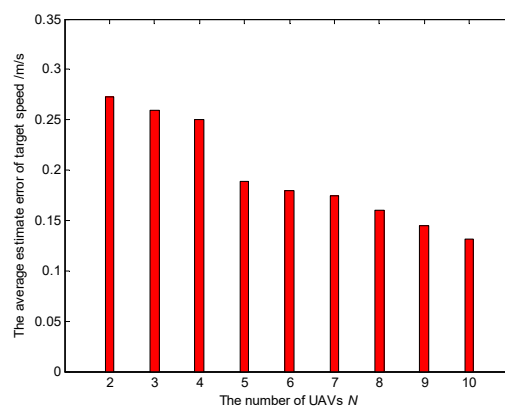

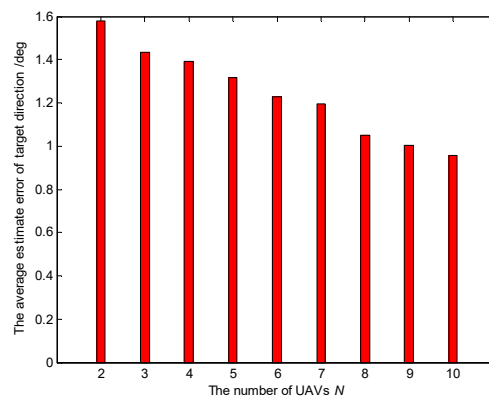**Figure 38.** The average estimation error of target speed for different numbers of UAVs (Scenario 5).

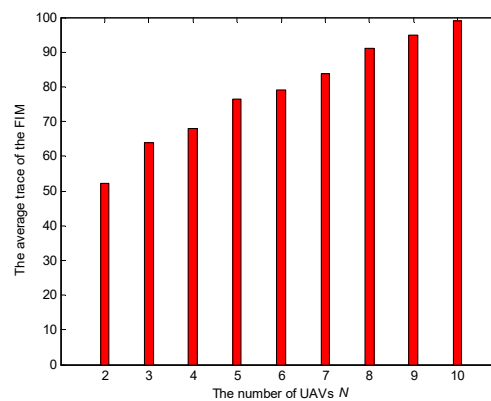**Figure 39.** The average estimation error of target direction for different numbers of UAVs (Scenario 5).

Figure 40. The average trace of the FIM for different numbers of UAVs (Scenario 5).

6. Conclusions

The problem of multiple UAVs cooperative tracking of a ground moving target is studied. The main contribution of this paper is to develop a motion planning algorithm in which communication and sensing are both optimized. This novel motion planning approach properly integrates the communication and sensing objectives to accomplish the target tracking mission of the multiple UAVs, while maintaining proper connectivity to the remote base station.

The performance of target fusion and estimation not only depend on overall information contained in given data sets of measurement of the UAVs, but also depend on whether the UAVs could successfully send their measurement packets back to the base station or not. According to this idea, the co-optimization of communication and sensing scheme is designed.

On one hand, a packet-erasure channel model is applied to model the communication links. In this channel model, the successful transmission probability is a function of the SNR, which is regarded as the communication reliability. On the other hand, the FIM is used to quantify the information gained by observation from the UAVs in target tracking process, which is regarded as the sensing utility. The communication reliability and the sensing utility are combined into a single utility function, which is used to plan trajectories over a finite time horizon for the UAVs. To maximize the overall information gain delivered to the base station, each UAV must make a tradeoff between maximizing the information gain through sensing and improving the probability of a successful transmission with the base station. The results of comparison simulations show that the proposal approach could improve fusion and estimation performance compared to method that does not consider communication optimization.

To produce efficient results in the moving target tracking scenario, the topology optimization strategy based on the minimum spanning tree (MST) is designed. The MST communication topology determines the planning hierarchy, which is the order of the optimization calculation in the distributed frame. Compared to the fix communication topology strategy, the results of simulations verify the rationality and validity of the topology optimization strategy.

Author Contributions: Conceptualization, Z.L. and X.F.; Methodology, Z.L.; Software, Z.L.; Validation, Z.L., X.G. and X.F.; Formal Analysis, X.F.; Investigation, Z.L.; Resources, X.F.; Data Curation, Z.L.; Writing-Original Draft Preparation, Z.L.; Writing-Review & Editing, Z.L.; Visualization, Z.L.; Supervision, X.F.; Project Administration, X.G.; Funding Acquisition, X.G.

Conflicts of Interest: The authors declare no conflict of interest.

References

1. Fu, X.W.; Liu, K.P.; Gao, X.G. Multi-UAVs communication-aware cooperative target tracking. *Appl. Sci.* **2018**, *8*, 870. [CrossRef]
2. Zhou, Z.; Fang, H.; Hong, Y. Distributed estimation for moving target based on state-consensus strategy. *IEEE Trans. Autom. Control* **2013**, *58*, 2096–2101. [CrossRef]
3. Fu, X.W.; Bi, H.Y.; Gao, X.G. Multi-UAVs cooperative localization algorithms with communication constraints. *Math. Probl. Eng.* **2017**, 1943539. [CrossRef]
4. Wang, Y.; Zheng, W.; Sun, S.; Li, L. Robust information filter based on maximum correntropy criterion. *J. Guid. Control Dyn.* **2016**, *39*, 1126–1131. [CrossRef]
5. Fu, X.W.; Feng, H.C.; Gao, X.G. UAV Mobile ground target pursuit algorithm. *J. Intell. Robot. Syst.* **2012**, *68*, 359–371. [CrossRef]
6. Lu, K.L.; Zhou, R.; Li, H. Event-triggered cooperative target tracking in wireless sensor networks. *Chin. J. Aeronaut.* **2016**, *29*, 1326–1334. [CrossRef]
7. Ridley, M.; Nettleton, E.; Göktogan, A.; Brooker, G.; Sukkarieh, S.; Durrant-Whyte, H.F. Decentralized ground target tracking with heterogeneous sensing nodes on multiple UAVs. In *Information Processing in Sensor Networks*; Springer: Berlin/Heidelberg, Germany, 2003; pp. 545–565.
8. Casbeer, D.W.; Beard, R. Distributed information filtering using consensus filters. In Proceedings of the American Control Conference, St. Louis, MO, USA, 10–12 June 2009; pp. 1882–1887.
9. Wang, L.; Li, Y.; Zhu, H.; Shen, L. Target state estimation and prediction based standoff tracking of ground moving target using a fixed-wing UAV. In Proceedings of the 8th IEEE International Conference on Control and Automation (ICCA), Xiamen, China, 9–11 June 2010; pp. 273–278.
10. Chung, T.H.; Burdick, J.W.; Murray, R.M. A decentralized motion coordination strategy for dynamic target tracking. In Proceedings of the IEEE Conference on Robotics and Automation, Orlando, FL, USA, 15–19 May 2006; pp. 2416–2422.
11. Yang, P.; Freeman, R.A.; Lynch, K.M. Distributed cooperative active sensing using consensus filters. In Proceedings of the IEEE Conference on Robotics and Automation, Roma, Italy, 10–14 April 2007; pp. 405–410.
12. Frew, E.W.; Lawrence, D.A.; Steve, M. Coordinated standoff tracking of moving targets using Lyapunov guidance vector fields. *J. Guid. Control Dyn.* **2008**, *31*, 290–306. [CrossRef]
13. Oh, H.; Kim, S.; Shin, H.S.; Tsourdos, A. Coordinated standoff tracking of moving target groups using multiple UAVs. *IEEE Trans. Aerosp. Electron. Syst.* **2015**, *51*, 1501–1514. [CrossRef]
14. Ponda, S.S.; Kolacinski, R.M.; Frazzoli, E. Trajectory optimization for target localization using small unmanned aerial vehicles. In Proceedings of the AIAA Guidance, Navigation and Control, Chicago, IL, USA, 10–13 August 2009; pp. 1–25.
15. Wang, L.; Su, F.; Zhu, H.; Shen, L. Active sensing based cooperative target tracking using UAVs in an urban area. In Proceedings of the IEEE International Conference on Advanced Computer Control, Shenyang, China, 27–29 March 2010; pp. 486–491.

16. Cao, Y.; Yu, W.; Ren, W.; Chen, G. An overview of recent progress in the study of distributed multi-agent coordination. *IEEE Trans. Ind. Inform.* **2012**, *9*, 427–438. [CrossRef]

17. Calvo, J.A.L.; Alirezaei, G.; Mathar, R. Wireless powering of drone-based MANETs for disaster zones. In Proceedings of the IEEE International Conference on Wireless for Space and Extreme Environments, Montreal, QC, Canada, 10–12 October 2017; pp. 98–103.

18. Stachura, M.; Frew, E.W. Cooperative target localization with a communication-aware unmanned aircraft system. *J. Guid. Control Dyn.* **2011**, *34*, 1352–1362. [CrossRef]

19. Olfati-Saber, R.; Murray, R.M. Graph rigidity and distributed formation stabilization of multi-vehicle systems. In Proceedings of the IEEE Conference on the Decision and Control, Las Vegas, NV, USA, 10–13 December 2002; pp. 2965–2971.

20. Nelson, D.R.; Barber, D.B.; McLain, T.W.; Beard, R.W. Vector Field Path Following for Miniature Air Vehicles. *IEEE Trans. Robot.* **2007**, *23*, 519–529. [CrossRef]

21. Michael, N.; Mellinger, D.; Lindsey, Q.; Kumar, V. The GRASP Multiple Micro-UAV Testbed. *IEEE Robot. Autom. Mag.* **2010**, *17*, 56–65. [CrossRef]

22. Park, S.; Deyst, J.; How, J.P. Performance and Lyapunov stability of a nonlinear path-following guidance method. *J. Guid. Control Dyn.* **2007**, *30*, 1718–1728. [CrossRef]

23. Fu, X.W.; Gao, X.G. Effective real-time unmanned air vehicle path planning in presence of threat netting. *J. Aerosp. Inf. Syst.* **2014**, *11*, 170–177. [CrossRef]

24. Zhu, H.; Swindlehurst, A.; Liu, K. Optimization of MANET connectivity via smart deployment/movement of unmanned air vehicles. *IEEE Trans. Veh. Technol.* **2009**, *58*, 3533–3546. [CrossRef]

25. Liu, Z.; Gao, X.G.; Fu, X.W. A cooperative search and coverage algorithm with controllable revisit and connectivity maintenance for multiple unmanned aerial vehicles. *Sensors* **2018**, *18*, 1472. [CrossRef] [PubMed]

26. Flocchini, P.; Enriquez, T.M.; Pagli, L.; Prencipe, G.; Santoro, N. Distributed minimum spanning tree maintenance for transient node failures. *IEEE Trans. Comput.* **2012**, *61*, 408–414. [CrossRef]